TRAJECTORY-BASED OBSTACLE AVOIDANCE AND PILOT CUEING VIA 3D CONFORMAL SYMBOLOGY IN DEGRADED VISUAL ENVIRONMENTS

Ceren Cansu Esmek
Graduate Student

Rahul Tauro-Padival
Undergraduate Student

Karen M. Feigh
Professor

J.V.R. Prasad
Professor

Vertical Lift Research Center of Excellence
Georgia Institute of Technology
Atlanta, GA, U.S.

ABSTRACT

Low situational awareness (SA) when operating close to terrain and obstacles significantly increases risk by dramatically reducing reaction times. This study aims to facilitate real-time trajectory adjustments and improve pilot SA without increasing cognitive load by focusing on the specific challenge of maneuvering around obstacles in hostile and degraded visual environments (DVE). This methodology aims to enhance the safety and efficiency of low-altitude rotorcraft operations. This study proposes an outer-loop guidance methodology and decision logic to facilitate a smooth transition between turn, climb, and deceleration maneuvers under appropriate circumstances during flight. Several desktop simulations are performed in the MATLAB/Simulink environment using different pilot models to test the performance in terms of obstacle avoidance and mission completion within the specified time interval. The primary objective of these studies is to lay the groundwork for future pilot-in-the-loop simulations by designing a framework to integrate this guidance method into a simulator, where visual cues are presented as a 3D conformal symbology set using a Heads-Up Display (HUD) to support the 'heads-up, eyes-out' interface philosophy. The proposed 3D conformal symbology set is explained. This preliminary work is intended to enhance the potential effectiveness of the pilot's cueing system in hostile and degraded visual environments once actual testing and implementation are underway.

NOTATION

*

Symbols

t time, s

g Gravitational acceleration, ft/s^2

$U(t)$ Closing velocity on the obstacle, ft/s

$X(t)$ Distance from an obstacle, ft

τ time-to-collision (or time-to-contact), s

$\dot{\tau}$ rate of change of τ

τ_m margin value of τ, s

$\dot{\tau}_m$ margin value of $\dot{\tau}$

φ_{cmd} Bank Angle Guidance

χ_{cmd} Heading Angle Guidance

ROC_{cmd} Rate of Climb Guidance

γ_{cmd} Flight Path Angle Guidance

$|\vec{V_G}^I|$ Ground Speed

*

Acronyms

DI Dynamic Inversion

DVE Degraded Visual Environment

ERITS Equivalent Retreating Indicated Tip Speed

FPA Flight Path Angle

HUD Heads-Up Display

LTI Linear Time-Invariant

ROC Rate of Climb

SA Situational Awareness

TITS Tunnel-in-the-Sky

INTRODUCTION

Obstacle avoidance is a widely studied problem for all types of controllable dynamic systems, with solutions developed over the years using various methods: optimal trajectory generation (Ref. 1), panel method-based path planning (Ref. 2), pilot cueing (Ref. 3), and others (Refs. 4–9). Binet and Rakotomamonjy (Ref. 3) developed an obstacle avoidance methodology using the Tau theory (Ref. 10), which was used to establish haptic cueing by generating a force bias on the lateral cyclic. Inspired by this work (Ref. 3), a bank angle guidance method based on Tau theory was proposed for obstacle avoidance (Ref. 10) in (Ref. 11). This study presents a method for generating a bank angle guidance to enable a pilot to make a coordinated turn away from an obstacle and safely change the helicopter's trajectory to avoid a collision. In this method, the altitude and speed of the rotorcraft are maintained, and it is assumed that the obstacle has infinite height, restricting the methodology to the two-dimensional (2D) plane. Therefore, additional adjustments are required to extend the method to a three-dimensional (3D) space.

Padfield (Ref. 12) explains that when pilots approach obstacles, they have three options: turn away, climb over, or stop before reaching the obstacle. For time-critical missions, stopping is the least favorable option, as it risks compromising mission completion. In DVE conditions, the pilot may be advised to decelerate if the bank angle or rate of climb command exceeds the helicopter's operational limits. To improve safety at low altitudes or in degraded visual environments, an algorithm with three guidance methods has been developed: bank angle guidance, climb rate guidance, and deceleration guidance, along with decision logic for smooth transitions between them to help pilots avoid obstacles in DVE conditions. While the bank angle guidance method introduced in (Ref. 11) addresses obstacle avoidance in the 2D plane, the rate of climb guidance extends this capability to the 3D space. Additionally, deceleration guidance and decision logic that integrates these methods are further elaborated in (Ref. 13). Tau Theory (Ref. 10) forms the foundation for developing the algorithms that generate the bank angle, rate of climb, and deceleration guidance. The deceleration guidance algorithm, which calculates the deceleration trajectory while keeping the rate of change of τ constant, is based on Lee's (Ref. 10) investigation of how time-to-collision information influences visual control of braking in traffic. Once the deceleration trajectory is generated, it is transformed into pitch angle guidance through dynamic inversion (DI), as described in (Ref. 14). Finally, the decision logic, shown in (Ref. 13), completes the algorithm, ensuring smooth transitions between guidance methods based on desktop simulations that test the individual performance of the bank angle and rate of climb guidance algorithms. This ensures that the helicopter stays within its operational limits while safely navigating around obstacles. Within the scope of this study, several desktop simulations were conducted to evaluate the performance of the methodology in terms of obstacle avoidance and mission completion within the specified time interval. Both the LTI model, extracted using the FLIGHTLAB generic helicopter model, and the nonlinear model were used for this purpose. The simulations were conducted in the MATLAB/Simulink environment, utilizing pilot models that represented both experienced and inexperienced pilots. These pilot models, based on the crossover model (Ref. 15), were used to issue commands throughout the simulations. These simulations indicate that the mission can be completed without hitting the obstacle, while maintaining a target mission duration for most experimental cases.

This research considers an approach to rotorcraft cueing that integrates time with spatial visualization to provide pilots with an intuitive and comprehensive understanding of their immediate flight environment and trajectory. The goal is to provide pilots with a dynamic and predictive view of their environment, enabling them to make informed decisions quickly and safely by adopting a four-dimensional (4D) perspective. This approach is particularly relevant in DVE conditions. Since the obstacle avoidance guidance algorithm is designed to be implemented as a 4D conformal pilot cueing system, a 3D conformal symbology set is required. Therefore, the three visual cues comprising all the guidance algorithms have been proposed in (Ref. 13). Figures 1 and 2 provide a visual representation of the developed cue symbology. The bank angle cue and pitch angle cue symbology are inspired by standard flight directors. The bank angle cue indicates the required bank angle for a coordinated turn maneuver that clears an obstacle, while the pitch angle cue shows the necessary pitch angle to decelerate to the extent needed in executing a turn maneuver within limits. The cue is visually represented by two wing-like bars connected by a semicircle, while the helicopter's actual bank and pitch angles are depicted by a bar with a central circle that can fit within the gap of the aforementioned cue. Pilots follow the obstacle avoidance cue by aligning the attitude indicator bar with the cue indicator bar. When the bank angle cue is active, the wing-like bars tilt left or right; when the pitch angle cue is generated, they move up or down. These cues are successfully followed when the pilot maintains the bar within the cue indicator bar. Both the cueing symbology set and attitude indicators are centrally positioned on the head-up display (HUD) at the pilot's eye level. The rate of climb cue indicates the required climb rate to clear an obstacle without collision. This symbology is represented by a green cylinder overlaid on the Vertical Speed Indicator on the right side of the HUD, with markings indicating a maximum climb rate of 4,000 feet per minute (fpm). The height of the cylinder expands as the rate of climb cue increases. As the helicopter increases its climb rate to match the rate of climb cue, the Vertical Speed Indicator bar follows the green cylinder. Finally, the safety zone cue outlines a no-go zone extending to 30 ft above the obstacle's height, visually indicating the area that must be avoided. The implementation of the symbology set in the Unreal Engine world is illustrated in Figures 1 and 2. In Figure 1, the helicopter approaches the obstacle from a lower level, causing the bank angle cue to be activated. In Figure 2, the helicopter approaches the same obstacle from a higher level, so the rate of climb cue is activated. In both figures, the safety zone can be seen around the obstacle. The orange arrows on the figures indicate the symbols.

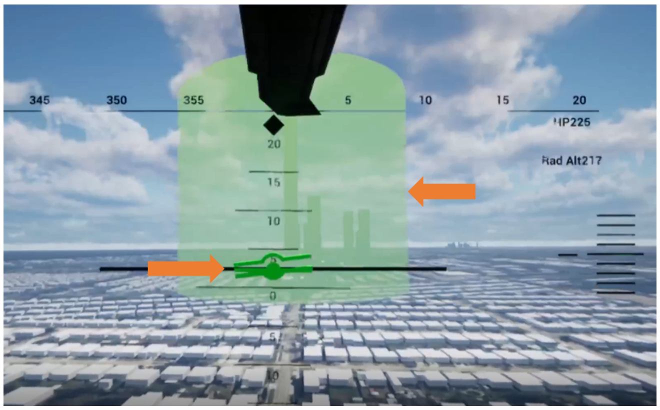

Figure 1. Bank angle and pitch angle cue and safety zone shown in a footage of preliminary pilot-in-the-loop testing in the GT high-fidelity, fixed-base rotorcraft flight simulator

Figure 2. Rate of climb cue shown in a footage of preliminary pilot-in-the-loop testing in the GT high-fidelity, fixed-base rotorcraft flight simulator

Although inner-loop guidance, which includes bank angle, pitch angle, and rate of climb guidance, performs well in desktop simulations using a pilot model, unofficial pilot interviews indicate that it is highly time-sensitive, leaving pilots with almost no reaction time. This increases workload and necessitates an outer-loop guidance set for three maneuvers: turn, climb, and decelerate. To address this, a novel outer-loop guidance method is developed in this study. As in the development phase of the inner-loop guidance, the outer-loop guidance is also first tested on the desktop using the same pilot models. In this paper, a 3D conformal visual cueing set has been proposed comprising all the outer-loop guidance algorithms to be tested in the GT high-fidelity, fixed-base rotorcraft flight simulator. The goal is to be able to show the pilot a preview of the intended trajectory.

METHODOLOGY

The outer-loop guidance methodology, which involves three obstacle avoidance maneuvers — turning, climbing, and deceleration —is explained in the following sections.

Outer Loop Guidance

The outer-loop guidance consists of heading angle guidance for turning, flight path angle guidance for climbing, and deceleration trajectory guidance for reducing the vehicle speed.

Heading Angle Guidance The heading angle guidance, χ_{cmd}, is found using the bank angle guidance, (Refs. 11, 13), as shown in Eq. 1.

$$\chi_{cmd} = \frac{tan(\varphi_{cmd})\tau g}{|\vec{V}_G^{\,I}|} \tag{1}$$

Flight Path Angle Guidance The flight path angle guidance, γ_{cmd}, is found by using the rate of climb guidance, (Ref. 13), as shown in Eq. 2.

$$\gamma_{cmd} = \frac{ROC_{cmd}}{|\vec{V}_G^{\,I}|} \tag{2}$$

Trajectory Guidance for Deceleration The purpose of the deceleration trajectory guidance is to follow the commanded deceleration velocity given in Eq. 3 during climbing or turning in obstacle avoidance maneuvers. It is the outer-loop form of the pitch angle guidance (Ref. 13).

$$U(t) = U(0)\left(1 + \frac{\dot{\tau}_m U(0)t}{X(0)}\right)^{-1-\frac{1}{\dot{\tau}_m}} \tag{3}$$

Since $U(t)$ is along the line-of-sight between the vehicle and the obstacle, the component of $U(t)$ along the x-axis of the body-fixed frame should be used as u_{cmd}.

Decision Logic

A decision-making algorithm is implemented to determine whether a helicopter should perform a climb or turn maneuver to avoid detected obstacles, while staying within its operational limits. The process begins by detecting all obstacles within a specified range from the helicopter's current position. For each obstacle, the algorithm calculates its relative position and evaluates its proximity in horizontal and vertical directions.

In this study, guidance algorithms are developed for speeds higher than 60 knots. Different guidance algorithms should be used for low-airspeed flight ($\leq$40 knots).

Turn Maneuver Evaluation The decision logic evaluates all obstacles on the helicopter's trajectory and selects the closest obstacle with the steepest required flight path angle (FPA) for which a climb maneuver is not possible within τ seconds, using the excess power at the best climb rate speed. This obstacle becomes a hard constraint, requiring a turn maneuver. The required flight path angle to avoid obstacles by climbing is determined by examining the horizontal and vertical distances to the helicopter.

The turn guidance is generated by identifying the closest gap that is wide enough for the helicopter to pass through. In other words, if there is an obstacle that the helicopter must turn to avoid, all the obstacles around it are checked, and the safest and closest heading to turn to is found.

In high-speed flight, the turning maneuver is mainly limited by the retreating blade stall. Therefore, the Equivalent Retreating Indicated Tip Speed (ERITS) parameter is checked at each time step during the turn maneuver to avoid the retreating blade stall. If the ERITS parameter is less than the selected value for the onset of the retreating blade stall, then the deceleration guidance is initiated.

Limited by Rotor Stall The ERITS parameter is an empirical metric developed by Sikorsky to support real-time rotor stall detection in helicopters. It is defined as in Eq. 4.

$$\text{ERITS} = \left(\Omega R\sqrt{\frac{\rho}{\rho_{SL}}} - V_i\right)\sqrt{\frac{W_0}{N_z W}} \tag{4}$$

where W_0 is a nominal reference weight, W is the current aircraft weight, N_z is the load factor, ρ is the air density at the flight altitude, ρ_{SL} is the standard sea-level air density, Ω is the rotor angular speed, R is the rotor radius, and V_i is the indicated airspeed. The derivation of the ERITS expression is given in (Ref. 16). The ERITS parameter correlates inversely with the lift coefficient at the retreating blade tip at approximately 270° azimuth, under the simplifying assumption of a uniform lift distribution across the blade. As such, a low ERITS value is expected to indicate a high retreating blade lift coefficient, which can be a precursor to retreating blade stall. Although the parameter is physics-based, the threshold for detecting stall, i.e., the ERITS limit, is empirically determined. This approach has been shown to be conservative, sometimes indicating stall in conditions where none is observed, particularly in maneuvers where dynamic blade interactions complicate the interpretation of control loads. Nevertheless, the simplicity of ERITS makes it a practical parameter for onboard implementation, especially when augmented with additional context such as altitude or load factor adjustments (Refs. 16, 17).

Climb Maneuver Evaluation After determining that a direct climb over the steepest obstacle is not feasible, the algorithm evaluates other obstacles that are closer to the helicopter. For each such obstacle, the required flight path angle is computed, and the system identifies the one with the steepest FPA that the helicopter might still be able to clear.

The algorithm then checks whether the available excess power is sufficient to achieve the required climb in τ seconds. If not, it assesses whether sufficient excess power can be recovered through deceleration, based on the approximation that the power required for forward flight scales with the cube of airspeed above the best climb rate speed. If deceleration enables the helicopter to generate the required excess power, the deceleration guidance is initiated. If deceleration still does not yield sufficient excess power, then the next closest obstacle, requiring the next steepest FPA, becomes the new hard constraint requiring a turn maneuver.

At each time step, all maneuvers required to avoid detected obstacles on the helicopter's trajectory are recalculated from the beginning, taking into account the current flight condition and all detected obstacles.

Limited by Engine Power To climb a vertical distance ΔH, the required gravitational potential energy is given by:

$$E_{\text{required}} = W\Delta H \tag{5}$$

To achieve this climb in τ seconds, the required average power is:

$$P_{\text{required}} = \frac{E_{\text{required}}}{\tau} \tag{6}$$

The available excess power is computed as:

$$P_{\text{excess}} = 0.9\,\eta_{\text{engine}}\left(Q_{\max} - Q_{\text{engine}}\right)\Omega_{\text{engine}} \tag{7}$$

where η_{engine} is the engine efficiency, $Q_{\max}$ is the maximum continuous torque, Q_{engine} is the current engine torque, and Ω_{engine} is the engine power turbine angular speed. It is assumed that approximately 90% of the total engine power is delivered to the main rotor.

If $P_{\text{required}} > P_{\text{excess}}$, the system evaluates whether the necessary excess power can be recovered through deceleration. This is approximated by assuming that the power required to maintain forward flight scales with the cube of airspeed above the best climb rate speed. If deceleration yields sufficient excess power to meet P_{required}, the deceleration guidance is initiated.

DESKTOP SIMULATIONS

To test the performance of the methodology in terms of obstacle avoidance and mission completion within the specified time interval capability, several desktop simulations were performed. FLIGHTLAB® nonlinear generic helicopter model is used for this purpose. The simulations are performed in the MATLAB/Simulink environment. Pilot models representing different pilots are used to complete the simulations. The pilot models based on the crossover model (Refs. 15, 18) are used to give commands. The transfer function of the pilot model is given in Eq. 8, where K_p is the pilot gain, T_L and T_I are lead-lag time constants, and τ^e is the time delay. These parameters for each pilot are selected as listed in Table 1.

$$Y_p(s) = K_p \frac{1+T_L s}{1+T_I s}.e^{-\tau_e s} \tag{8}$$

Table 1. Pilot models.

Pilot	T_L **[s]**	T_I **[s]**	τ_e **[s]**
Pilot A	0.2	0.2	0.2
Pilot B	0.1	0.3	0.3

The architecture of the pilot model consists of four input channels. The following control architecture is used for the outer-loop simulations:

- In the collective channel, the cascaded controller structure is used. The outer loop controls the flight path angle, and the inner loop controls the vertical speed.
- In the pedal channel, the pilot model achieves zero lateral acceleration.
- The longitudinal cyclic channel uses the cascaded controller structure. The deceleration trajectory guidance is followed in the outer loop. The inner loop controls the pitch angle.
- In the lateral cyclic channel, the cascaded controller structure is used. The outer loop controls the heading angle, and the inner loop controls the bank angle.

Lead-lag time constants and time delay are kept at zero except for the inner loops in the four input channels. The outer-loop controller architecture is given in Figure 3.

The gains of the outer-loop pilot models used in this study are given in Table 2. Gains of the outer-loop pilot models are selected arbitrarily to achieve successful obstacle avoidance maneuvers with minimal control movements and without compromising stability.

Table 2. Outer-loop controller gains.

K_{P1}	K_{P2}	K_{P3}	K_{P4}	K_{P5}	K_{P6}	K_{P7}
1	-15	30	50	150	-0.01	2

Simulation Results and Discussion

Desktop simulations begin with 80 knots forward flight trim conditions with zero sideslip. These simulations are performed using the "Pilot A" pilot models. In all simulations, the mission is plotted as the helicopter moves from

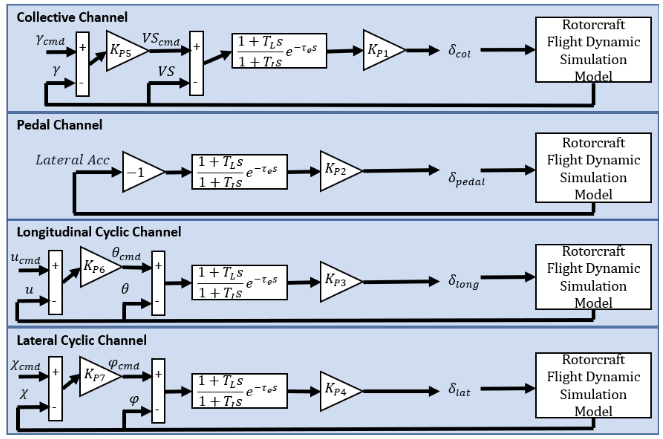

Figure 3. Outer-loop controller architecture.

$(x_I, y_I) = (0,0)$ ft coordinates in the inertial frame at 150 ft altitude to the target point $(x_I, y_I) = (12000, 0)$ ft coordinates in the inertial frame at 150 ft altitude. The number, size, and location of obstacles are kept as variables, generating different terrain scenarios. In the simulations, the radius of the sphere surrounding the helicopter is set to 50 ft. Finally, τ_m is fixed to 30 seconds; in other words, the obstacle avoidance algorithm starts working when the time-to-impact is less than 30 seconds.

The results of the simulation performed for the outer-loop guidance from the top, side, and isometric views are shown in Figures 4, 5, and 6, respectively. For this simulation, the obstacle specifications are given in Table 3. The obstacle numbers can be seen in Figures 4, 5, and 6.

Table 3. Obstacle data.

Obstacle Number	**Radius [ft]**	**Height [ft]**	**Location** (x_I, y_I) **[ft]**
1	200	200	(4500, 0)
2	350	600	(6500, -50)
3	250	400	(8500, 100)
4	400	800	(10500, -50)

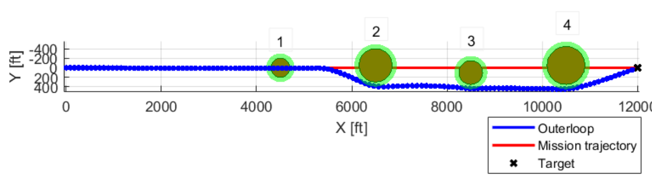

Figure 4. Top view of the obstacle avoidance trajectory.

Figures 7 and 8 show the obstacle avoidance maneuvers, as well as turn, climb, and deceleration commands for outer-loop guidance simulations. It also illustrates the obstacles that are avoided by performing these maneuvers. Figures 9, 10, 11, and 12 show the helicopter response in all four channels.

As shown in Figures 7–12, the helicopter performs three types of obstacle avoidance maneuvers while navigating toward the

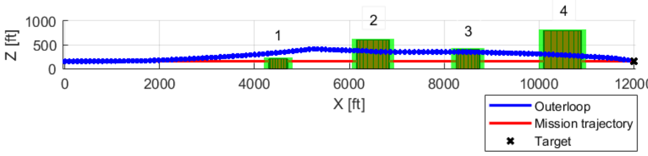

Figure 5. Side view of the obstacle avoidance trajectory.

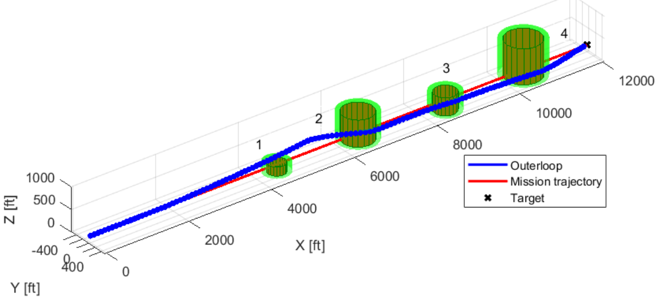

Figure 6. Isometric view of the obstacle avoidance trajectory.

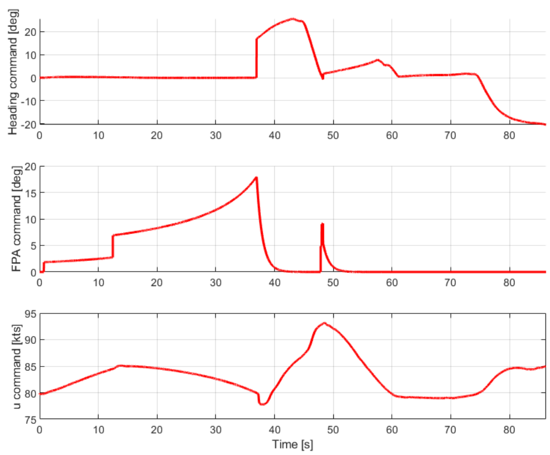

Figure 7. Outer-loop guidance turn-climb-deceleration commands.

target: turning, climbing, and decelerating. It first initiates a climb maneuver to avoid Obstacle #1. Then, it attempts to climb over Obstacle #2; however, even with deceleration, this becomes infeasible as the helicopter approaches the obstacle. Because the helicopter does not perfectly follow the commanded flight path angle, as illustrated in Figure 9, it is unable to complete the climb in the remaining τ seconds. Consequently, at around 38 seconds, the system initiates a turn maneuver to avoid Obstacle #2. The helicopter then encounters Obstacles #3 and #4. It briefly attempts to climb over Obstacle #4, but this also proves infeasible. As a result, it first turns to avoid Obstacle #3, then again to avoid Obstacle #4. Ultimately, the helicopter reaches the target successfully at 86 seconds.

As the purpose of the desktop simulations is to prepare the algorithm for seamless simulator integration, it can be concluded that, according to these results, the methodology provides a promising solution for low-altitude, high-

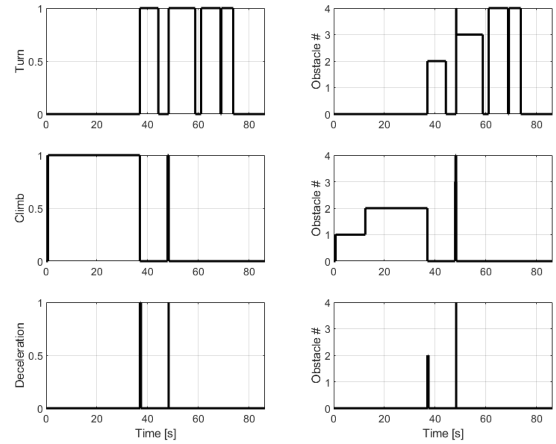

Figure 8. Outer-loop guidance obstacle avoidance maneuvers and the obstacle numbers that are avoided.

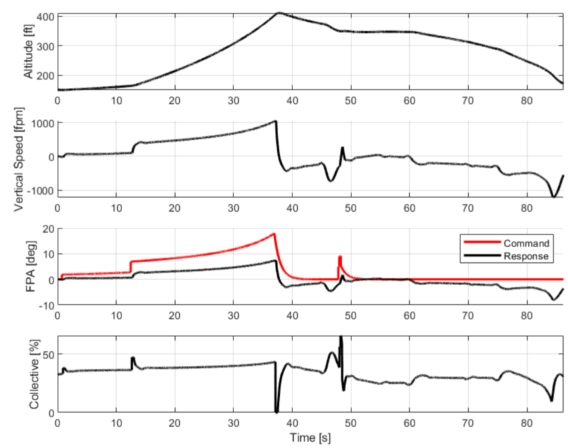

Figure 9. Outer-loop guidance responses in collective channel.

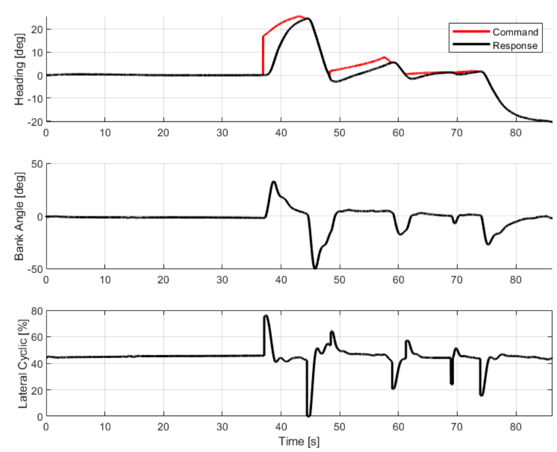

Figure 10. Outer-loop guidance responses in lateral cyclic channel.

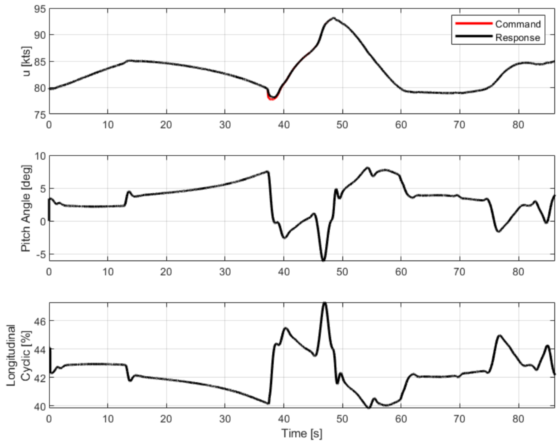

Figure 11. Outer-loop guidance responses in longitudinal cyclic channel.

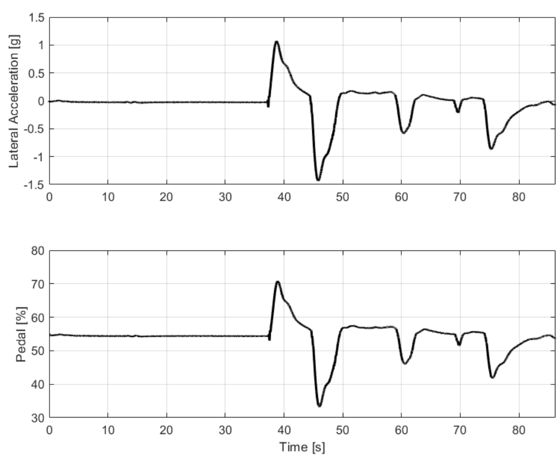

Figure 12. Outer-loop guidance responses in pedal channel.

speed terrain-following flights, especially in obstacle-dense, degraded visual environments. The actual performance of the methodology can be assessed through pilot-in-the-loop simulations. Additionally, although the decision logic works well in desktop simulations, it can be further refined by incorporating pilots, as determined by the requirements identified during the pilot-in-loop tests.

DESCRIPTION OF 3D CONFORMAL SYMBOLOGY

The following 3D conformal symbologies are proposed for use in visualizing the outer-loop guidance. Their performance will be tested in GT high-fidelity, fixed-base rotorcraft flight simulator. The simulation environment for initial tests is created in Unreal Engine 5.1 environment. The simulation environment consists of obstacles of various sizes, realistic terrain imported from the Cesium plugin, and a UH60 helicopter model found on the Epic Games Marketplace.

Tunnel in the Sky

Tunnel-in-the-Sky (TITS) displays provide pilots with a spatial visualization of future 4D flight paths, aiding in trajectory conformance and situational awareness during complex approaches. Compared to conventional 2D formats, these perspective displays reduce cognitive load and improve control precision by intuitively integrating lateral, vertical, and temporal information (Refs. 19, 20). Foundational work by Theunissen, Mulder, and Wickens has shown that well-designed TITS symbology can significantly enhance performance and safety in future airspace environments (Refs. 21–23). TITS supports both turning and climbing trajectories, providing pilots with a clear, predictable path for safer and more efficient maneuvering, as it dynamically adjusts in real-time. For this study, equally-spaced, color-coded octagons represent the TITS. Distance between the frames and the color of the frames changes according to τ. Table 4 shows the intervals of τ and corresponding colors and distances.

Table 4. Tunnel-in-the-sky

τ [s]	Color	Distance (x) [m]
0–5	Red	50
5–15	Amber	70
> 15	Blue	90

The heading angle guidance is used to generate the horizontal position of the intended trajectory, and the flight path angle guidance is used to generate the vertical position of the intended trajectory.

$$X_{tr} = x_i cos(\chi_{cmd}) \tag{9}$$

$$Y_{tr} = x_i sin(\chi_{cmd}) \tag{10}$$

$$Z_{tr} = x_i sin(\gamma_{cmd}) \tag{11}$$

Equations 9, 10, and 11 give the x_I, y_I, and z_I coordinates of the trajectory in the inertial frame over a x ft distance of commanded trajectory. The subscript ”i” represents the i-th frame, starting with the closest one.

TITS symbology is accompanied by predictor symbology and flight path vector symbology, both with the same color-coding shown in Table 4. Predictor symbology is placed in the middle of the closest frame, showing the midpoint both vertically and horizontally, which enables easier frame following. The flight path vector is placed on the same plane as the closest frame and shows the current heading and flight path angle of the helicopter. Coinciding the predictor and the flight path vector ensures accurate frame following. The symbologies are shown in Figure 14.

Three variations of the TITS symbology will be evaluated via objective and subjective testing. One version will have an altitude bar placed beneath the frames, and the frames will be straight. The second version will be curved without an altitude bar, and the third version will be straight without an altitude bar. A banked flight path vector is employed when curved tunnel symbology is used. Different variations of TITS symbology are shown in Figures 13-17.

Figure 13. TITS symbology with altitude bar, $5 < \tau < 15$.

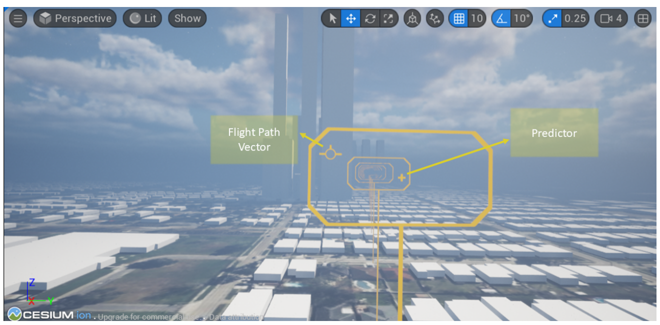

Figure 14. Zoomed-in TITS symbology with altitude bar shown together with predictor and flight path vector symbologies, $5 < \tau < 15$.

Figure 15. Curved TITS symbology without altitude bar, $5 < \tau < 15$.

Path Marker Cubes

In addition to TITS symbology, path marker cubes can be used to show the intended trajectory. Path marker cubes serve as spatial reference indicators along the desired trajectory path. They mark intermediate waypoints or time-delayed predictions of the aircraft's position in space. The cubes appear as

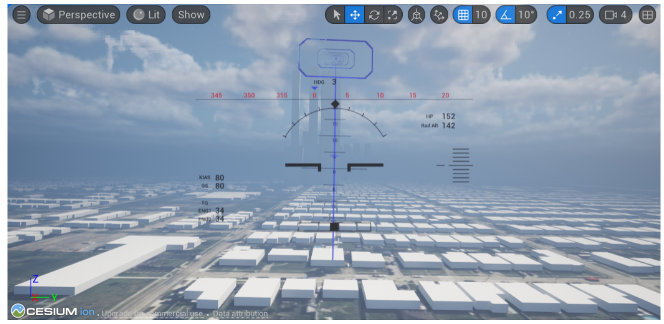

Figure 16. TITS symbology with altitude bar, $\tau > 15$.

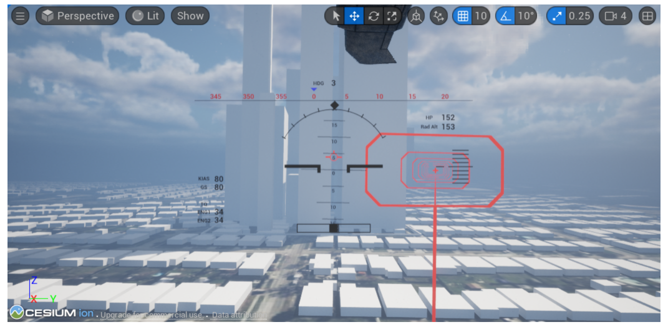

Figure 17. TITS symbology with altitude bar, $\tau < 5$.

solid or semi-transparent geometric markers that guide the pilot visually, (Ref. 24). In this study, path marker cubes are placed on two sides of the TITS at every 10 m distance. The cubes have the same color-coding shown in Table 4. The effect of combining the TITS and path marker cube symbology will be evaluated. Combination of the two symbologies are shown in Figures 18-20.

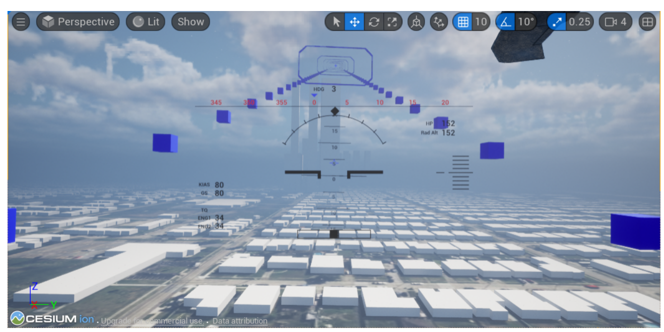

Figure 18. Combination of TITS without altitude bar and path marker cubes symbologies, $\tau > 15$.

Speed Error Ladder

To visualize the trajectory guidance for deceleration, a speed error ladder is employed, (Ref. 24). This way, as the error between the speed guidance and the helicopter's speed increases, the penny moves on the ladder, indicating the need for deceleration. If the helicopter is too fast, the penny moves away from the helicopter and gets closer to the red vertical bar. If the penny is in the middle, on the green vertical bar, then the helicopter does not need to decelerate. The symbology and

Figure 19. Combination of curved TITS without altitude bar and path marker cubes symbologies, $5 < \tau < 15$.

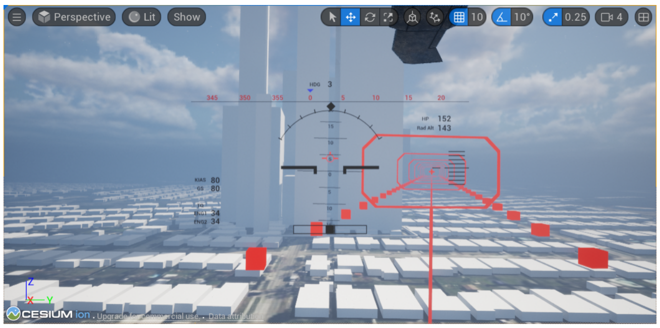

Figure 20. Combination of TITS with altitude bar and path marker cubes symbologies, $\tau < 5$.

how the penny moves on the ladder are illustrated in Figures 21, 22.

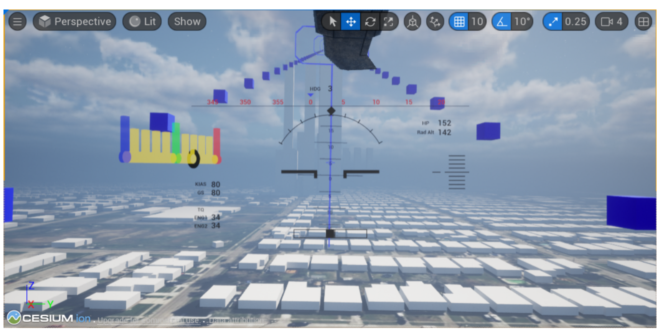

Figure 21. Speed error ladder symbology: The helicopter is 4 knots faster.

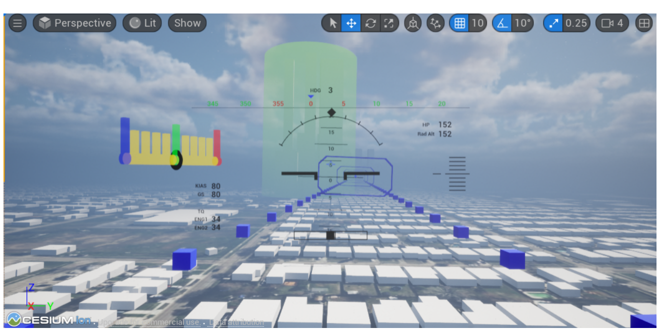

Figure 22. Speed error ladder symbology, no deceleration is needed.

CONCLUSIONS

1. An outer-loop guidance methodology was developed for helicopter obstacle avoidance that integrates turning, climbing, and deceleration maneuvers, guided by a decision logic framework. This framework evaluates maneuver feasibility based on available excess power and aerodynamic limits.

2. A decision-making algorithm was implemented to evaluate all obstacles on the trajectory, determine the most suitable avoidance strategy, and execute smooth transitions between maneuvers while maintaining the aircraft within operational limits.

3. A 3D conformal symbology set was designed to visualize the guidance commands through intuitive visual cues, including Tunnel-in-the-Sky, path marker cubes, and a speed error ladder. These symbologies aim to reduce cognitive workload and improve situational awareness in degraded visual environments.

4. Desktop simulations using FLIGHTLAB-based nonlinear helicopter models and pilot transfer function models confirmed the feasibility of the methodology for dynamic, terrain-following, low-altitude flight. The system demonstrated successful mission completion and effective obstacle avoidance across varied terrain scenarios.

5. The methodology is ready for integration into a high-fidelity, fixed-base rotorcraft flight simulator environment, where it will be tested through pilot-in-the-loop experiments to assess usability, workload, and operational performance in more realistic conditions.

FUTURE WORK

Future work will focus on conducting pilot-in-the-loop experiments using the developed 3D conformal symbology set within the GT high-fidelity, fixed-base rotorcraft flight simulator. These experiments aim to evaluate the usability, intuitiveness, and cognitive workload associated with the symbology, and to assess the effectiveness of the outer-loop guidance system in dynamic flight scenarios under degraded visual conditions. Additional refinements to the decision logic are planned based on feedback from pilot testing, with a focus on improving timing sensitivity and maneuver prioritization. Finally, extending the framework for fully autonomous obstacle avoidance or optionally-piloted vehicle (OPV) applications represents a promising avenue for broader operational deployment.

Author contact: Ceren Cansu Esmek ccesmek@gatech.edu,
Rahul Tauro-Padival rahulpadival@gatech.edu,
Karen M. Feigh karen.feigh@gatech.edu,
J. V. R. Prasad jvr.prasad@gatech.edu

ACKNOWLEDGMENTS

This research was partially funded by the U.S. Government under Cooperative Agreement No. W911W6-21-2-0001. The U.S. Government is authorized to reproduce and distribute reprints for Government purposes notwithstanding any copyright notation thereon. The views and conclusions contained in this document are those of the authors and should not be interpreted as representing the official policies of position, either expressed or implied, of the U.S. Army Combat Capabilities Development Command (DEVCOM), Aviation & Missile Center (AvMC), or the U.S. Government.

REFERENCES

1. Kang, K., Prasad, J., and Dhingra, M., "Simulation Evaluation Of An Adaptive Optimal Multiple Obstacle Avoidance Algorithm For Autonomous UAVs," Proceedings of the American Helicopter Society 67th Annual Forum, 2011.

2. Unal, Z., and Yavrucuk, I., "Panel-Method-Based Path Planning for eVTOL in Urban Environment," Proceedings of the Vertical Flight Society 77th Annual Forum, 2021.

3. Binet, L., and Rakotomamonjy, T., "Using Haptic Feedbacks For Obstacle Avoidance In Helicopter Flight," Proceedings of the 6th European Conference for Aeronautics and Space Sciences (EUCASS), 2015.

4. Rakotomamonjy, T., Binet, L., and Müllhäuser, M., "ONERA-DLR Joint Research On Tactile Cueing For Reactive Obstacle Avoidance Dedicated To Low Speed Helicopter Maneuvers," Proceedings of the 44th European Rotorcraft Forum, 2016.

5. Walko, C., and Müllhäuser, M., "Design Of A Haptic Obstacle Avoidance For Low-Speed Helicopter Operations Using Active Sidesticks," *The Aeronautical Journal*, 2023, pp. 1–17.

6. Godfroy-Cooper, M., Miller, J. D., Szoboszlay, Z., and Wenzel, E. M., "3D-Sonification for Obstacle Avoidance in Brownout Conditions," Proceedings of the 73th American Helicopter Society Annual Forum Technology Display, 2017.

7. Godfroy-Cooper, M., Miller, J. D., Bachelder, E., and Wenzel, E. M., "Isomorphic Spatial Visual-Auditory Displays For Operations In DVE For Obstacle Avoidance," Proceedings of the 44th European Rotorcraft Forum, 2018.

8. Miller, J. D., Godfroy-Cooper, M., and Wenzel, E. M., "ARSAD: An Augmented-Reality Spatial Auditory Display for Obstacle Avoidance for all Phases of Flight," Proceedings of the 74th American Helicopter Society Annual Forum Technology Display, 2018.

9. Miller, J. D., Godfroy-Cooper, M., and Szoboszlay, Z. P., "Augmented-Reality Multimodal Cueing for Obstacle Awareness: Towards a New Topology for Threat-Level Presentation," Proceedings of the 75th American Helicopter Society Annual Forum Technology Display, 2019.

10. Lee, D. L., "A Theory of Visual Control of Braking based on Information about Time-to-Collision," *Perception*, Vol. 5, 1976, pp. 437–459.

11. Kwon, J., Esmek, C., Tauro-Padival, R., Feigh, K., and Prasad, J., "4D Conformal Pilot Cueing for Rotorcraft Army Operational Scenarios," Proceedings of the Vertical Flight Society 80th Annual Forum Technology Display, 2024.

12. Padfield, G. D., "The Tau of Flight Control," *The Aeronautical Journal*, Vol. 115, 2011, pp. 521–556.

13. Esmek, C., Tauro-Padival, R., Feigh, K., and Prasad, J., "Tau-theory-based Visual Cueing Method for Obstacle Avoidance," Proceedings of the 50th European Rotorcraft Forum, 2024.

14. Saetti, U., Rogers, J., Alam, M., and Jump, M., "Tau Theory-Based Flare Control in Autonomous Helicopter Autorotation," *Aerospace*, Vol. 11,33, 2024.

15. McRuer, D. T., and Jex, H. R., "A Review of Quasi-Linear Pilot Models," *IEEE Transactions on Human Factors in Electronics*, Vol. HFE-8, 1967, pp. 231–249.

16. Grill, I., Dhingra, M., and Prasad, J., "Methods for Real-Time Rotor Stall Detection," Proceedings of the 34th European Rotorcraft Forum, 2008.

17. Grill, I., Dhingra, M., and Prasad, J., "Analysis of Real-Time Rotor Stall Detection Methods," Proceedings of the American Helicopter Society 65th Annual Forum, 2009.

18. Friesen, D., Pavel, D. M., Borst, C., Masarati, P., and Mulder, M., "Pilot Model Development And Human Manual Control Considerations For Helicopter Hover Displays," Proceedings of the 45th European Rotorcraft Forum, 2019.

19. Theunissen, E., *Integrated Design of a Man-Machine Interface for 4-D Navigation*, Ph.D. thesis, Delft University of Technology, 1997.

20. Haskell, I., and Wickens, C., "Two- and Three-Dimensional Displays for Aviation: A Theoretical and Empirical Comparison," *The International Journal of Aviation Psychology*, Vol. 3, (2), 1993, pp. 87–109. DOI: 10.1207/s15327108ijap0302$_1$.

Theunissen, E., "A Primary Flight Display for 4-D Guidance and Navigation," AIAA Guidance, Navigation, and Control Conference, 1993.

22. Mulder, M., *Cybernetics of Tunnel-in-the-Sky Displays*, Ph.D. thesis, Delft University of Technology, 1999.

23. Doherty, B., and Wickens, C., "An Analysis of the Immersed Perspective Flightpath Display Benefit," *The International Journal of Aviation Psychology*, Vol. 10, (3), 2000, pp. 247–271. DOI: 10.1207/S15327108IJAP1003$_4$.

24. Walters, R., *Augmented Reality Cueing Methodologies for Rotorcraft Shipboard Landings*, Ph.D. thesis, Georgia Institute of Technology, Ph.D. dissertation detailing the development of the 3D FPM cue and path marker cubes across multiple experimental phases, 2022.

CLASSIFICATION & COPYRIGHT